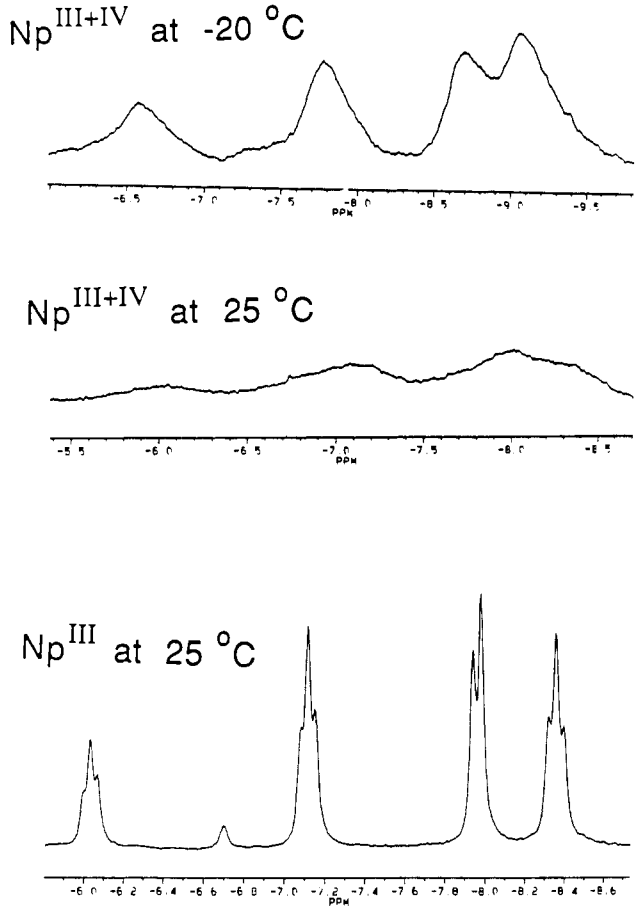

Figure 6. ^{1}H NMR spectra of ring protons in potassium bis(*tert*-butyl[8]annulenediyl)neptunate(III) and its mixture with 1,1′-di-*tert*-butylneptunocene.

that was available for this transuranium work of about 9000 Hz. This is almost twice as large as the difference in the previously studied ytterbium system. Unfortunately, this spectrometer is only equipped to go down to −20 °C, but at that temperature the ring peaks do sharpen considerably as can be seen in Figure 6, indicating that the slow-exchange region has almost been reached.

These results, although not as quantitative as desired, do nevertheless demonstrate that the rates of electron exchange between actinide(III) and actinide(IV) derivatives of cyclooctatetraene are on the same order of magnitude as those for the ytterbium system.[1] The former case may be considered as involving electron tranfser between an ion pair (the potassium bis([8]annulenediyl)actinide(III) salt) and a neutral actinide(IV) compound, whereas the ytterbium exchange involves an ion pair (the potassium bis([8]annulenediyl)ytterbate(III) salt) and a triple ion (the dipotassium bis([8]annulenediyl)ytterbate(II) salt). In both systems, however, electron exchange is accompanied by transfer of a potassium cation. This cation probably requires partial desolvation in the exchange transition state, a feature in ion aggregate electron exchange systems that complicates the possible application of Marcus theory.[1] The fast exchange found for the present cases does nevertheless demonstrate a commonality of exchange processes for both actinide and lanthanide f-element systems.

Conclusions

Electron transfers in THF between the III and IV oxidation states of the [8]annulene sandwich compounds of uranium, neptunium, and plutonium are rapid on the NMR time scale and appear to be qualitatively comparable to the exchange between the ytterbium(II) and -(III) oxidation states studied previously.[1]

Acknowledgment. This work was supported by the Director, Office of Energy Research, Office of Basic Energy Sciences, Chemical Sciences Division of the Department of Energy, under Contract No. DE-AC03-76SF00098. We also thank Dr. Phillip G. Williams for assistance with the NMR spectra of the transuranium compounds, which were all run at the National Tritium Labeling Facility, Lawrence Berkeley Laboratory.

Registry No. K[U(C_8H_8)$_2$], 124020-90-2; K[U(MeC_8H_7)(C_8H_8)], 124020-91-3; K[Pu(t-BuC_8H_7)$_2$], 124020-94-6; K[Np(t-BuC_8H_7)$_2$], 124020-95-7; uranocene, 11079-26-8; methyluranocene, 124020-89-9; bis(tetraethylammonium)neptunium(IV) hexachloride, 12080-88-5; *tert*-butylcyclooctatetraene, 61593-18-8; 1,1′-di-*tert*-butylneptunocene, 124020-92-4; 1,1′-di-*tert*-butylplutonocene, 124020-93-5; bis(tetraethylammonium)plutonium(IV) hexachloride, 33393-76-9.

Contribution from the Exxon Research and Engineering Company, Annandale, New Jersey 08801

Conversion of $[MoS_4]^{2-}$ to $[Mo_2S_2(\mu\text{-}S)_2(S_2)_2]^{2-}$ by Organic Disulfides: The Mechanism of an Induced Redox Reaction

C. L. Coyle,* M. A. Harmer, G. N. George, M. Daage, and E. I. Stiefel*

Received September 7, 1988

The kinetics of the reaction of tetrathiomolybdate, $[MoS_4]^{2-}$, with organic disulfides, RSSR, to produce the Mo(V) dimer $[Mo_2S_2(\mu\text{-}S)_2(S_2)_2]^{2-}$ have been investigated. The reaction involves an internal redox process and occurs in two stages. The overall rate of reaction is dependent on the electron-withdrawing properties of the disulfide such that diphenyl disulfide < bis(*p*-chlorophenyl) disulfide < bis(*p*-carboxyphenyl) disulfide. The first stage involves rapid equilibrium formation of an EPR-inactive, green intermediate. The reaction of $[MoS_4]^{2-}$ with diphenyl disulfide or bis(*p*-chlorophenyl) disulfide is first order in tetrathiomolybdate and first order in organic disulfide. However, the reaction of $[MoS_4]^{2-}$ with bis(*p*-carboxyphenyl) disulfide is more complex. Analysis of the molybdenum X-ray absorption spectrum of the green intermediate indicates the likelihood of a mononuclear species with two to three short Mo–S interactions at 2.16 Å and three to four longer Mo–S interactions at 2.41 Å. The rate-determining step of the second stage of the reaction involves first-order rearrangement or dissociation of the green intermediate. This is followed by rapid reaction of the resultant complex with another molybdenum species to produce $[Mo_2S_2(\mu\text{-}S)_2(S_2)_2]^{2-}$. Mechanisms are proposed that are consistent with these findings and that provide potential insight into the use of oxidants to prepare new lower valent transition-metal sulfur-containing complexes from tetrathiometalate starting materials.

Transition-metal sulfur-containing sites in enzymes and heterogeneous catalysts undergo redox during catalysis.[1-3] Although many of these redox reactions are metal-centered, some involve processes that are localized on the sulfur ligands.[4,5] Moreover,

0020-1669/90/1329-0014$02.50/0 © 1990 American Chemical Society

there are a few examples wherein both the metal and the sulfur ligands participate in the redox reaction.[6,7] The mechanistic understanding of such redox reactions is complicated, as internal electron-transfer processes are often involved and these can be difficult to monitor directly.

The reaction of tetrathiomolybdate, $[MoS_4]^{2-}$, with elemental sulfur to produce $[MoS(S_4)_2]^{2-}$, (eq 1), first reported by Coucouvanis and co-workers,[8] is particularly interesting. Here

$$[Mo^{VI}S_4]^{2-} + \tfrac{5}{8}S_8 \rightarrow [Mo^{IV}S(S_4)_2]^{2-} \quad (1)$$

$[MoS_4]^{2-}$, containing hexavalent Mo(VI), is "oxidized" quantitively by elemental sulfur to produce via internal redox a reduced Mo(IV) species. Similarly, the reaction of the two-electron oxidant RSSR with tetrathiomolybdate also results in reduction of the Mo(VI) metal center to produce the Mo(V) dimer, $[Mo_2S_2(\mu\text{-}S)_2(S_2)_2]^{2-}$, as shown in (2).[9] The kinetics and mechanism of reaction 2 are the focus of this paper.

$$2(NH_4)_2MoS_4 + RSSR \rightarrow (NH_4)_2[Mo_2S_2(\mu\text{-}S)_2(S_2)_2] + 2(NH_4)RS \quad (2)$$

Reaction 2 involves internal electron transfer from sulfur to molybdenum that is induced by the addition of the external oxidant RSSR. Induced internal redox processes have been described previously in a few other reactions.[10,11] One of the most notable of these was analyzed by Taube and co-workers[12] in the reaction of $[Co^{III}(NH_3)_4(C_2O_4)]^+$ with Ce(IV) shown in (3). In this

$$[Co^{III}(NH_3)_4(C_2O_4)]^+ + Ce(IV) \rightarrow Co(II) + Ce(III) + 2CO_2 \quad (3)$$

reaction, the Ce(IV) acts as an external one-electron oxidant and induces an intramolecular one-electron transfer from oxalate to Co(III). The net effect is the reduction of Co(III) to Co(II) and the oxidation of the oxalate ligand by two electrons to carbon dioxide. Kinetic studies were carried out to establish mechanistic details.[12] Here we use kinetic studies to probe the mechanism of an induced redox process involving a transition-metal sulfide complex.

Experimental Section

All solvents and reagents were used as obtained unless stated otherwise. Kinetic studies were done under anaerobic conditions. Ammonium tetrathiomolybdate, $(NH_4)_2[MoS_4]$, was purchased from SPEX and tetraethylammonium tetrathiomolybdate, $(Et_4N)_2[MoS_4]$, was prepared as previously described.[13] Dimethylformamide (DMF) was glass-distilled grade and obtained from Burdick and Jackson. The bis(*p*-carboxyphenyl) disulfide, PCDD, was purchased from ICN Pharmaceuticals, Inc., and recrystallized from DMF/acetonitrile.

The slow reactions were monitored on a Perkin-Elmer Model 330 UV–vis spectrophotometer equipped with a temperature-control unit. Fast reactions were monitored with a Dionex Model D-110 stopped-flow spectrophotometer interfaced by Olis to a Northstar minicomputer. Electron paramagnetic resonance (EPR) measurements were made by using a Varian Model E-109 spectrometer.

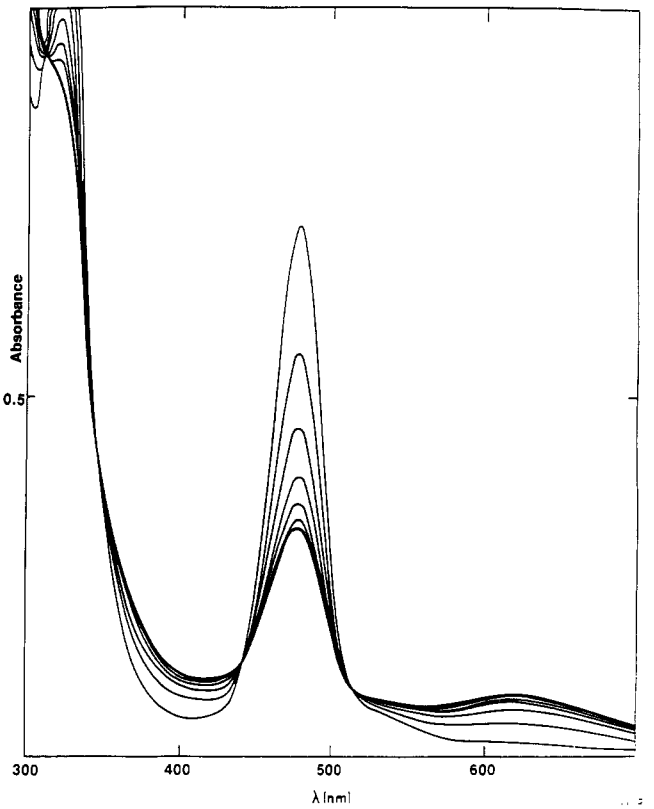

Figure 1. Electronic spectra as a function of time for the first stage of the reaction of $(NH_4)_2[MoS_4]$ with PhSSPh (5×10^{-4} M) at 25 °C in DMF to form the green intermediate (ca. 15 min to reach completion).

X-ray absorption data were collected at the Stanford Synchrotron Radiation Laboratory on beam line IV-2 using a Si(220) crystal monochromator with the electron storage ring SPEAR operating in dedicated mode (40–70 mA at 3 GeV). X-ray absorption was detected as the fluorescence excitation spectrum by using a Stern–Heald–Lytle ion chamber detector[14] containing krypton gas. During data collection, samples were maintained at a temperature close to 4 K in an Oxford Instruments CF204 liquid-helium flow cryostat. The energy scale was calibrated with reference to the first inflection point of a molybdenum foil standard, which was assumed to be 20003.9 eV.

The EXAFS spectra $\chi(k)$ were quantitatively analyzed by curve fitting to the following approximate expression:

$$\chi(k) \simeq \sum_b \frac{N_b A_b(k)}{kR_{ab}^2} e^{-2\sigma_{ab}^2 k^2} \sin [2kR_{ab} + \alpha_{ab}(k)]$$

where N_b is the number of b-type atoms at a distance R_{ab} from the absorber atom a, k is the photoelectron wave number, σ_{ab} is the root-mean-square deviation of R_{ab} (the Debye–Waller factor). $A_b(k)$ and $\alpha_{ab}(k)$ are the total amplitude and phase-shift functions, respectively. Values for these were obtained from model compound EXAFS data.[15]

Results and Discussion

The study of the redox process described in eq 1 for the reaction of $[MoS_4]^{2-}$ with organic disulfides is particularly attractive. The overall stoichiometry of the reaction was established as that shown in eq 1, and the structures of the reagents and products are known. The overall reaction rate is dependent on the organic disulfide used, showing that the external oxidant is required to induce the internal electron-transfer process. Further, $[Mo_2S_2(\mu\text{-}S)_2(S_2)_2]^{2-}$ is also produced when diphenyl diselenide, RSeSeR, is used as the external oxidant, indicating that all of the sulfur in the product originates from the tetrathiomolybdate reactants.[9] The product, $[Mo_2S_2(\mu\text{-}S)_2(S_2)_2]^{2-}$, is two electrons more oxidized than the two Mo reactants as shown in eq 4.

$$2[MoS_4]^{2-} \rightarrow [Mo_2S_2(\mu\text{-}S)_2(S_2)_2]^{2-} + 2e^- \quad (4)$$

(1) Harmer, M. A.; Halbert, T. R.; Pan, W.-H.; Coyle, C. L.; Cohen, S. A.; Stiefel, E. I. *Polyhedron* **1986**, *5*, 341.
(2) Stiefel, E. I. *Prog. Inorg. Chem.* **1977**, *22*, 1.
(3) Spence, J. T. *Coord. Chem. Rev.* **1983**, *48*, 59.
(4) Miller, K. F.; Bruce, A. E.; Corbin, J. L.; Wherland, S.; Stiefel, E. I. *J. Am. Chem. Soc.* **1980**, *102*, 5102.
(5) Halbert, T. R.; McGauley, K.; Pan, W.-H.; Czernuszewicz, R. S.; Stiefel, E. I. *J. Am. Chem. Soc.* **1984**, *106*, 1849.
(6) Pan, W.-H.; Leonowicz, M. E.; Stiefel, E. I. *Inorg. Chem.* **1983**, *22*, 672.
(7) Simhon, E. D.; Baenziger, N. C.; Kanatzidis, M.; Draganjac, M.; Coucouvanis, D. J. *J. Am. Chem. Soc.* **1981**, *103*, 1218.
(8) Draganjac, M.; Simhon, E.; Chan, L. T.; Kanatzidis, M.; Baenziger, N. C.; Coucouvanis, D. *Inorg. Chem.* **1982**, *21*, 3321.
(9) Pan, W.-H.; Harmer, M. A.; Halbert, T. R.; Stiefel, E. I. *J. Am. Chem. Soc.* **1984**, *106*, 460.
(10) Woods, M.; Sullivan, J. C.; Deutsch, E. *J. Chem. Soc., Chem. Commun.* **1975**, 749.
(11) (a) Jasim, K. S.; Chieh, C.; Mak, T. C. W. *Inorg. Chim. Acta* **1986**, *116*, 37. (b) Sakar, S.; Ansari, M. A. *J. Chem. Soc., Chem. Commun.* **1986**, *4*, 324.
(12) Taube, H. *Electron Transfer Reactions of Complex Ions in Solution*; Academic Press: New York, 1970; pp 73–98.
(13) Friesen, G. D.; McDonald, J. W.; Newton, W. E.; Euler, W. B.; Hoffman, B. M. *Inorg. Chem.* **1983**, *22*, 2202.
(14) Stern, E.; Heald, S. *Rev. Sci. Instrum.* **1979**, *50*, 1579.
(15) Cramer, S. P.; Whal, R.; Rajagopalan, K. V. *J. Am. Chem. Soc.* **1981**, *103*, 7721.

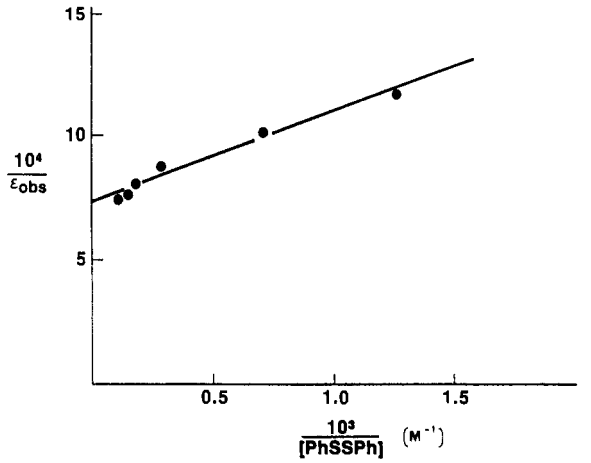

Figure 2. Determination of the equilibrium constant for the formation of the green intermediate from $(NH_4)_2[MoS_4]$(10^{-4} M) and PhSSPh (excess) in DMF at 25 °C. Double reciprocal plot of the observed absorption coefficient defined as the absorbance after complex formation divided by the initial concentration of $[MoS_4]^{2-}$ versus concentration of PhSSPh.

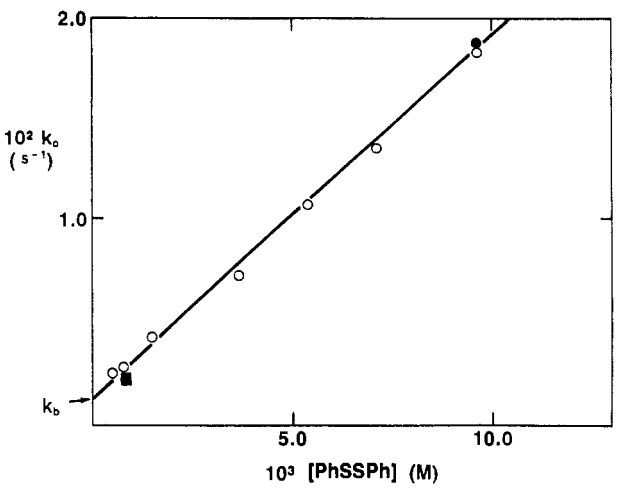

Figure 3. Dependence of the observed rate constant, k_0, on the concentration of PhSSPh for the first stage of the reaction of $(NH_4)_2[MoS_4]$ (10^{-4} M) with PhSSPh in DMF (λ = 470 nm, T = 25 °C) (○). Other points: (●) λ = 600 nm; (■) $[MoS_4]^{2-}$ = 8 × 10^{-2} M (excess) and [PhSSPh] = 10^{-4} M, λ = 600 nm.

Kinetics were monitored for the reaction with three organic disulfides: diphenyl disulfide, [PhSSPh], bis(*p*-chlorophenyl) disulfide, [(*p*-ClPhS)$_2$], and bis(*p*-carboxyphenyl) disulfide, PCDD. The overall rate of the reaction of $[MoS_4]^{2-}$ with these disulfides follows the order

$$PCDD > (p\text{-ClPhS})_2 > PhSSPh$$

The rate appears to depend on the electron-withdrawing capacity of the substituent on the phenyl ring.

In all cases, the reaction proceeds in two major stages. The first stage involves the rapid disappearance of the red-orange solution containing the $[MoS_4]^{2-}$ ion and the formation of a green intermediate. The second stage involves the disappearance of this green intermediate and the formation of purple $[Mo_2S_2(\mu\text{-}S)_2(S_2)_2]^{2-}$. Because of the distinctive colors of the reactant, intermediate, and product, the reaction is readily followed spectrophotometrically.

First Stage. The first stage of the oxidation of $[MoS_4]^{2-}$ by diphenyl disulfide is presented in Figure 1. The spectra were recorded at 3-min intervals. The formation of the green intermediate (λ_{max} = 620 nm) was maximal after approximately 15 min. The isosbestic points indicate that there are only two absorbing species present in solution. However, even with an excess of disulfide, the spectra indicate that an equilibrium concentration of $[MoS_4]^{2-}$ (λ_{max} = 470 nm) is present at the completion of this stage of the reaction. The equilibrium constant for this process was calculated from the double-reciprocal plot of the absorption coefficient versus the concentration of oxidant as shown in Figure 2. The reaction was monitored at 470 and 600 nm.

The dependence of the observed rate constant, k_0, on the concentration of oxidant for the first stage of the reaction of $[MoS_4]^{2-}$ with PhSSPh is shown in Figure 3. In these experiments, the disulfide is in a large (>10-fold) excess. The straight line indicates that the reaction is first order in disulfide.

Similar experiments were performed with the tetrathiomolybdate in a pseudo-first-order excess to confirm that the reaction is also first order in $[MoS_4]^{2-}$. The nonzero intercept is consistent with formulation of the first stage of this reaction as an equilibrium process as shown in (5). For this stage of the

$$[MoS_4]^{2-} + PhSSPh \underset{k_2}{\overset{k_1}{\rightleftharpoons}} I \text{ (green intermediate)} \quad (5)$$

reaction, where the concentration of PhSSPh or (*p*-ClPhS)$_2$ is in a pseudo-first-order excess, the observed rate, k_{obs}, can be expressed by eq 6. The kinetic data for the formation of the green inter-

$$k_0 = k_1[RSSR] + k_2 \quad (6)$$

mediate are summarized in Table I. The value of the equilibrium

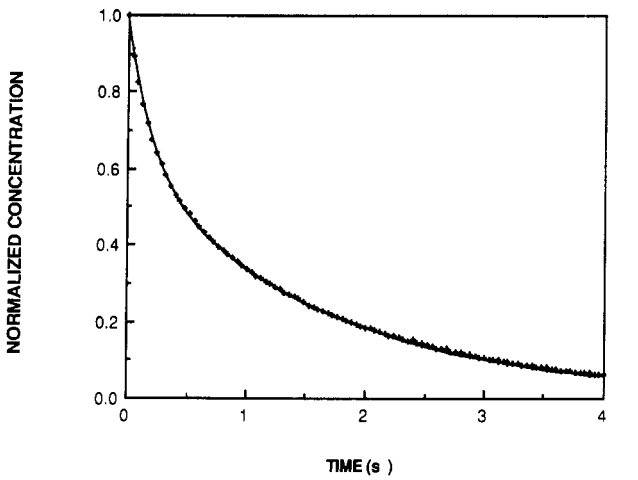

Figure 4. Variation of the normalized concentration as a function of time for the first stage of the reaction of $(NH_4)_2MoS_4$ (2.5 × 10^{-5} M) with PCDD (2.0 × 10^{-3} M) in DMF, (λ = 470 nm, T = 25 °C): (×) data; (—) best-fit curve.

Table I. Summary of Kinetic Data for the Formation of the Green Intermediate from the Reaction of $(NH_4)_2[MoS_4]$ and RSSR in DMF at 25 °C

$$(NH_4)_2[MoS_4] + RSSR \underset{k_2}{\overset{k_1}{\rightleftharpoons}} \text{green intermediate}$$

oxidant	k_1, M^{-1} s^{-1}	k_2, M^{-1} s^{-1}	K(kin)	K(spec)
PhSSPh	1.80	0.0012	1500	2000
(*p*-ClPhS)$_2$	26.0	<0.005	>6500	

$$(NH_4)_2[MoS_4] + RSSR \underset{k_2}{\overset{k_1}{\rightleftharpoons}} + (NH_4)[MoS_4(SR)] + (NH_4)SR$$

$$(NH_4)[MoS_4(SR)] + RSSR \underset{k_4}{\overset{k_3}{\rightleftharpoons}} \text{green intermediate}$$

oxidant	k_1, M^{-1} s^{-1}	k_2, M^{-1} s^{-1}	k_3, M^{-1} s^{-1}	k_4, M^{-1} s^{-1}
PCCD	0.1	1.8	0.017	0.008

constant obtained from these kinetic measurements is 1.5 × 10^3 M^{-1} as compared with the value 2.0 × 10^3 M^{-1} determined spectroscopically for the reaction of $[MoS_4]^{2-}$ with PhSSPh.

The equilibrium is shifted to the right as the substituent on the phenyl ring becomes more electron withdrawing. When PCDD is used as the organic disulfide, the reaction becomes more complicated and the data do not fit a simple first-order process, as shown in Figure 4. These data have been shown to fit the rate

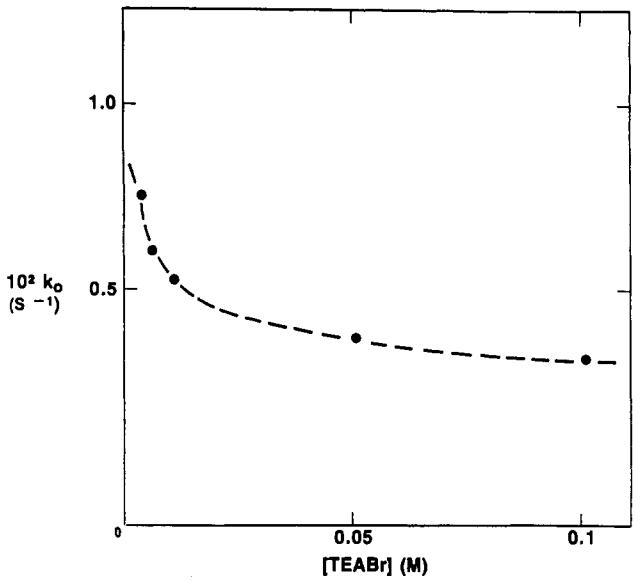

Figure 5. Variation of the observed rate constant, k_0, with ionic strength for the reaction of $(NH_4)_2[MoS_4]$ (10^{-4} M) with PhSSPh (3.6×10^{-3} M) in DMF at 25 °C and λ = 470 nm. The concentration of tetraethylammonium bromide is indicated by [(TEA)Br].

law described in (7) and plotted in Figure 4. A mechanism that is consistent with this rate law is presented in (8).

$$\frac{-d[MoS_4^{2-}]}{dt} = -k_1[MoS_4^{2-}][RSSR]^{0.7} + k_2[MoS_4(SR)^-] \quad (7)$$

$$(NH_4)_2[MoS_4] + RSSR \underset{k_2}{\overset{k_1}{\rightleftharpoons}} (NH_4)[MoS_4(SR)] + NH_4SR \quad (8a)$$

$$(NH_4)[MoS_4(SR)] + RSSR \underset{k_4}{\overset{k_3}{\rightleftharpoons}} \text{green intermediate} + NH_4SR \quad (8b)$$

The rate constants for this reaction are summarized in Table I. The best fit was obtained with the 0.7 order reaction of PCDD with $[MoS_4]^{2-}$, suggesting that the initial attack of $[MoS_4]^{2-}$ on PCDD is not a simple process. The reason for the more complicated kinetics for the reaction of tetrathiomolybdate with PCDD is uncertain; however, the protic nature of the carboxyl substituent on the phenyl ring may be responsible for hydrogen bonding to various other species in solution. One proposed mechanism would involve proton transfer and/or hydrogen bonding between $[MoS_4]^{2-}$ and the proton on the carboxyl group of PCDD in step 8a. This mechanism would also be consistent with the effect of ammonium ions described below.

The rate of the overall reaction of $[MoS_4]^{2-}$ with diphenyl disulfide to produce $[Mo_2S_2(\mu\text{-}S)_2(S_2)_2]^{2-}$ is dramatically affected by the cation associated with the tetrathiomolybdate anion. When this reaction is done at 90 °C on a preparative scale, the order of reactivity is

$$NH_4^+, Et_3NH^+ (\sim 1\ h) > Et_4N^+ (\sim 48\ h)$$

This appears to be a specific effect of the cation associated with the molybdenum complex anion, rather than a general proton effect, because the rate of the overall reaction is not significantly increased in the presence of acid.

The rate of the first stage of the reaction and the amount of green intermediate formed are dependent on the concentration of ammonium ions. When the concentration of ammonium ions is less than or equal to twice the concentration of $[MoS_4]^{2-}$, nonlinear log plots are obtained, indicating that the reaction is no longer simply first order in each of the reagents. The optimum rate of the reaction at constant ionic strength requires 2 equiv of ammonium ions. Further increases in the concentration of ammonium have no effect on the rate of the reaction. The effect of protons associated with the disulfide may also account for the different kinetics observed by using PCDD, because in this reaction there is an additional protic site associated with the oxidant.

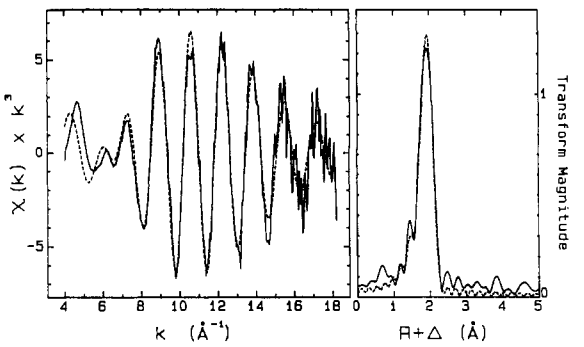

Figure 6. Molybdenum K-edge EXAFS plus best fit of the green intermediate. The left panel shows the EXAFS spectrum, and the right panel, the Fourier transform. The solid lines indicate experimental curves, and the broken lines, the best fit (Table II).

Table II. Green Intermediate EXAFS Curve-Fitting Results—Best Integer Fits[a]

N	R, Å	σ^2, Å^2	N	R, Å	σ^2, Å^2	error[b]
0			4	2.430	0.0047	8.175
2	2.148	0.0012	0			4.030
1	2.156	−0.0006	4	2.418	0.0057	2.302
2	2.156	0.0014	3	2.407	0.0036	0.968
3	2.156	0.0023	3	2.401	0.0031	1.016
2	2.157	0.0012	4	2.406	0.0053	1.274
3	2.157	0.0026	4	2.400	0.0046	1.127

[a] Values for R are considered accurate to ±0.02 Å. The k range dictates a resolution (the smallest discernible difference in R for two similar interactions) of approximately 0.09 Å. [b] The fit error function is defined as $\sum(\chi_o - \chi_c)^2k^6/n$, where n is the number of points in the fit and χ_o is the observed and χ_c the calculated EXAFS, where the summation is over all points.

The rate of formation of the green intermediate decreases as the ionic strength of the solution increases, which is consistent with the reaction of two oppositely charged species. Figure 5 illustrates this effect for the reaction with PhSSPh. The ammonium ion and ionic strength dependences are consistent with ion-pair formation with the possibility of specific proton transfer in the rate-limiting step of the reaction.

Attempts to isolate the green intermediate resulted in the production of a brown solid. This brown compound does not appear to be on the reaction pathway as it does not react further to produce $[Mo_2S_2(\mu\text{-}S)_2(S_2)_2]^{2-}$. The green intermediate shows no EPR signal at room temperature, indicating that it is probably not a monomeric Mo(V) species.

Analysis of the molybdenum X-ray absorption spectrum of the green intermediate is also consistent with the formulation of the species as a mononuclear Mo species with two different types of sulfur ligands. The molybdenum K edge EXAFS spectrum and EXAFS Fourier transform of the green intermediate are illustrated in Figure 6. The EXAFS Fourier transform shows only a single peak, with no long-range Mo–Mo interactions, indicating that the green intermediate is likely mononuclear. The EXAFS curve fitting analysis indicates the presence of two different first-shell Mo–S interactions; two to three at 2.16 Å and three to four at 2.41 Å (see Table II and Figure 6). From these results, we consider that a reasonable interpretation, with chemically appropriate Debye–Waller factors, is that the green intermediate is mononuclear and possesses two short (Mo–S) and four long (Mo–S) ligands.

Second Stage. The second stage of the reaction involves conversion of the green intermediate to the Mo(V) dimer $[Mo_2S_2(\mu\text{-}S)_2(S_2)_2]^{2-}$. The formation of $[Mo_2S_2(\mu\text{-}S)_2(S_2)_2]^{2-}$ is shown spectrophotometrically in Figure 7 for the oxidation by PCDD. Isosbestic points indicate the presence of $[Mo_2S_2(\mu\text{-}S)_2(S_2)_2]^{2-}$ (λ_{max} = 572 nm) and the green intermediate (λ_{max} = 610 nm) as the only two absorbing species in solution. This reaction appears first order even when a pseudo-first-order excess of disulfide is not maintained. The dependence of the observed rate constant,

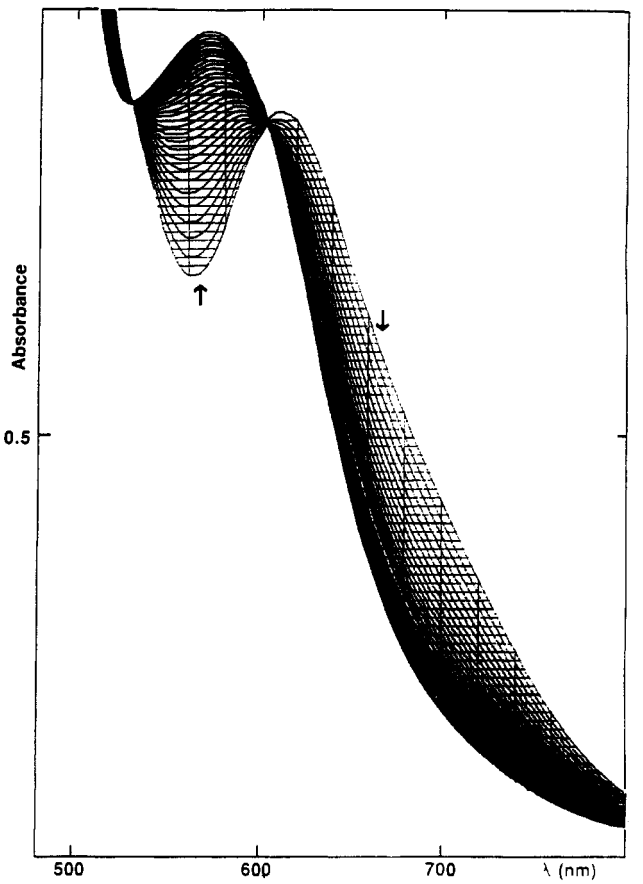

Figure 7. Absorption spectra of $(NH_4)_2[MoS_4]$(10^{-2} M) and PCDD (5 × 10^{-3} M) at 25 °C in DMF showing conversion of the green intermediate to $(NH_4)_2[Mo_2S_8]$ (ca. 4 h to reach completion).

k_0, on the concentration of disulfide, shown in Figure 8, reveals two distinct regions. In the first region, the concentration of disulfide is less than half the concentration of tetrathiomolybdate and the rate is independent of the concentration of disulfide. In the second region, the concentration of disulfide is greater than half the concentration of tetrathiomolybdate and the rate of the reaction is inversely proportional to the concentration of disulfide. This behavior is consistent with the mechanism shown in (9). If

stage 1

$$(NH_4)_2[MoS_4] + PCCD \underset{k_2}{\overset{k_1}{\rightleftharpoons}} (NH_4)[MoS_4(SR)] + NH_4SR \quad (9a)$$

$$(NH_4)[MoS_4(SR)] + PCCD \underset{k_4}{\overset{k_3}{\rightleftharpoons}} \text{green intermediate} + NH_4SR \quad (9b)$$

stage 2

$$\text{green intermediate} \xrightarrow[\text{slow}]{k_i} I^* \quad (9c)$$

$$I^* + (NH_4)_2[MoS_4] \xrightarrow[\text{fast}]{} (NH_4)_2[Mo_2S_2(\mu\text{-}S)_2(S_2)_2] + PCCD \quad (9d)$$

there is an excess of tetrathiomolybdate present, the rate of the reaction is independent of disulfide and the rate constant k_i is obtained. As the concentration of disulfide increases, the rate of the reaction decreases due to product inhibition by PCDD. Further, as the concentration of PCDD increases, the concentration of tetrathiomolybdate is decreased by reaction 9a, thereby decreasing the amount of tetrathiomolybdate available for reaction with **I*** to produce $[Mo_2S_2(\mu\text{-}S)_2(S_2)_2]^{2-}$. The rate constant for the formation of $[Mo_2S_2(\mu\text{-}S)_2(S_2)_2]^{2-}$ from the green intermediate at 25 °C is 1.86 × 10^4 s^{-1} for the reaction with PCDD. The activation parameters for this reaction have been determined from the temperature dependence of the rate. The activation enthalpy is +14.9 kcal/mol and the activation entropy is −26 cal/(mol deg).

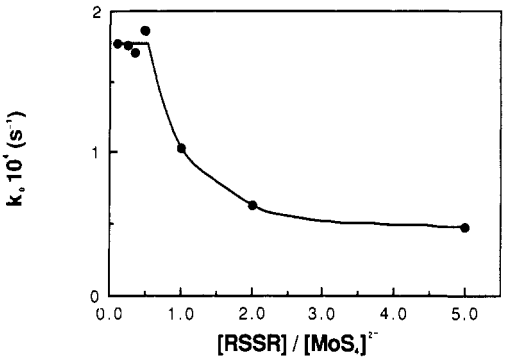

Figure 8. Variation of observed rate constant, k_0, for conversion of the green intermediate to $(NH_4)_2[Mo_2S_8]$ as a function of [PCDD] at fixed $[(NH_4)_2[MoS_4]]$ = 0.01 M in DMF (λ = 700 and 560 nm).

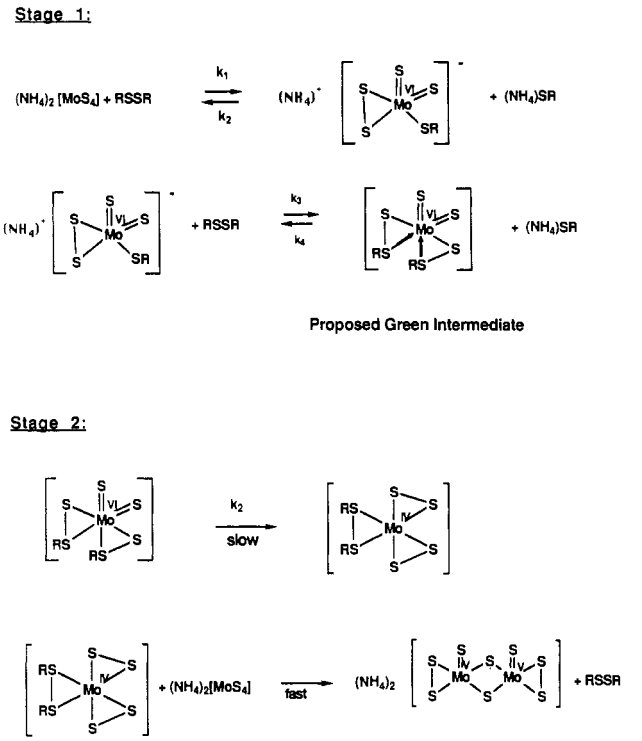

Figure 9. Proposed two-stage mechanism for the reaction of $(NH_4)_2[MoS_4]$ with organic disulfides, RSSR.

Mechanism. A suggested mechanism for the reaction that is consistent with the kinetic data is presented in Figure 9. The proposed mechanism involves initial attack of $[MoS_4]^{2-}$ on the disulfide, resulting in the formation of a mononuclear molybdenum species with two sulfide ligands. There is some precedent for this type of structure in the literature. The Mo(VI) monomers, $[MoO_2(dtc)_2]$[16] (**1**), $[MoOS(ONR_2)_2]$[17] (**2**), and $[MoS_2(ONR_2)_2]$[18] (**3**) have two cis oxide ligands, a cis oxide and sulfide ligand, and two cis sulfide ligands, respectively. Further, the W(VI) monomer $[WS(S_2)(dtc)_2]$[19] (**4**) has a terminal sulfide and a disulfide ligand.

The slow step of the second stage of the reaction may involve internal reduction of the Mo(VI) intermediate as shown in Figure 9. This slow step is proposed because the reaction was shown to be first order even without a pseudo-first-order excess of disulfide. The final fast step is required to account for the dinuclear nature of the product.

(16) Ricard, L.; Estienne, J.; Karagiannidis, P.; Toledano, P.; Fischer, J.; Mitschier, A.; Weiss, R. *J. Coord. Chem.* **1974**, *3*, 277.
(17) Bristow, S.; Collison, D.; Garner, C. D. *J. Chem. Soc., Dalton Trans.* **1983**, 2495.
(18) Wieghardt, V. K.; Hahn, M.; Weiss, J.; Swirdoff, W. *Z. Anorg. Allg. Chem.* **1982**, *492*, 164.
(19) Pan, W.-H.; Halbert, T. R.; Hutchings, L. L.; Stiefel, E. I. *J. Chem. Soc., Chem. Commun.* **1985**, *13*, 927.

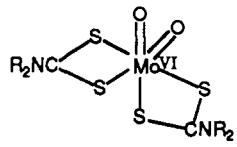

1

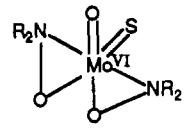

2

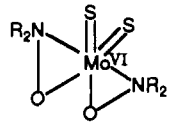

3

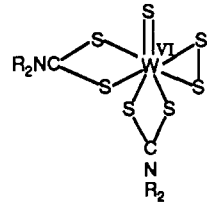

4

An alternate mechanism for the second stage of the reaction involves the anionic green intermediate (eq 10). This mechanism

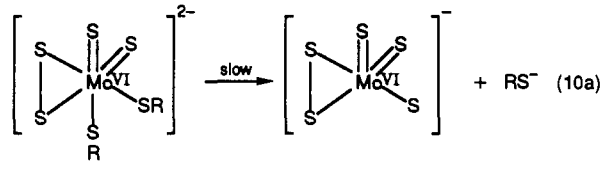

(10a)

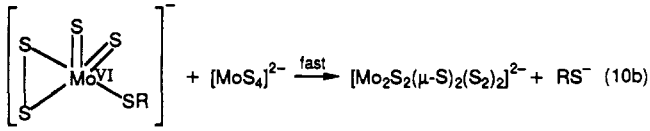

(10b)

invokes slow dissociation of thiolate to produce a monomeric Mo(VI) species. The final step of the reaction would then involve rapid attack on this species by $[MoS_4]^{2-}$ or another molybdenum complex followed by internal reduction to form $[Mo_2S_2(\mu\text{-}S)_2(S_2)_2]^{2-}$. The exact molybdenum oxidation states and structures of all of the intermediates are not known. An alternate structure for the green intermediate that is consistent with the kinetic and EXAFS data is **5**. This structure, as well as protonated forms

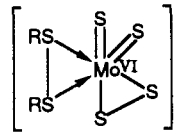

5

of the proposed intermediates, can not be ruled out. Further, there are no data regarding the timing of the loss of thiolate during the reaction. The last fast step in the reaction is proposed to involve reaction of the second intermediate, I*, with another molybdenum complex. This molybdenum species could be tetrathiomolybdate or any of the intermediates.

An understanding of this induced redox process has led to the synthesis of new transition-metal sulfur complexes. Since the proposed mechanism involves attack of $[MoS_4]^{2-}$ on disulfide followed by loss of thiolate, the use of disulfides of chelating ligands was explored.[19] The reaction of $[MoS_4]^{2-}$ with tetraalkylthiuram disulfides does not proceed to form $[Mo_2S_2(\mu\text{-}S)_2(S_2)_2]^{2-}$. Rather, the product is the monomeric $[MoS_2(dtc)_3]$.[19] Although the detailed kinetics of this reaction were not investigated, it is possible that the reaction proceeds by a mechanism similar to that of Figure 9. The isolation of a monomeric complex is consistent with the chelating dithiocarbamate ligand preventing the second stage of the reaction from proceeding by stabilizing the monomeric intermediate.

On the basis of this and other work,[1-3] it should no longer be considered unusual to react a higher valent molybdenum sulfur compound with an oxidant to produce a lower valent molybdenum sulfur compound. These reactions involve induced internal electron-transfer processes similar to the reaction whose mechanism is described in this paper. Moreover, such induced internal redox reactions have also been shown to occur with tungsten,[20] vanadium,[21] and rhenium complexes.[22]

Acknowledgment. We thank Drs. T. Halbert and L. Wei for helpful discussions and Drs. S. Cramer and R. Prince for their assistance with EXAFS data collection. X-ray absorption spectroscopy was done at the Stanford Synchrotron Radiation Laboratory, which is funded by the DOE, Office of Basic Energy Sciences, and the NIH Biotechnology Resource Program, Division of Research Resources.

Registry No. PCDD, 1155-51-7; $[MoS_4]^{2-}$, 16330-92-0; PhSSPh, 882-33-7; $(p\text{-ClPhS})_2$, 1142-19-4.

(20) Cohen, S. A.; Stiefel, E. I. *Inorg. Chem.* **1985**, *24*, 4657.
(21) Halbert, T. R.; Hutchings, L. L.; Rhodes, R.; Stiefel, E. I. *J. Am. Chem. Soc.* **1986**, *108*, 6437.
(22) Wei, L.; Halbert, T. R.; Stiefel, E. I. Manuscript in preparation.